


# Numerical study of heat transfer in circular pipe filled with porous medium

 The corrections made in this section will be reviewed by journal production editor.

Firas F. Qader<sup>1</sup>, Barhm Mohamad, PhD, <sup>2,\*</sup> [barhm.mohamad@epu.edu.iq](mailto:barhm.mohamad@epu.edu.iq), Adnan M. Hussein<sup>1</sup> and Suad H. Danook<sup>1</sup>

<sup>1</sup>Kirkuk Technical Engineering College, Northern Technical University, Kirkuk, Iraq

<sup>2</sup>Department of Petroleum Technology, Koya Technical Institute, Erbil Polytechnic University, Erbil, Iraq

\*Corresponding author. E-mail: [barhm.mohamad@epu.edu.iq](mailto:barhm.mohamad@epu.edu.iq)

## Abstract

Forced convection heat transfer was studied in a horizontally heated circular pipe with constant heat flux. Porous medium was created using 1 and 3 mm stainless-steel balls (porosity: 0.3690 and 0.3912). Reynolds numbers ranged from 3,200 to 6,500 based on pipe diameter, with heat flux rates of 6,250 and 12,500 W m<sup>-2</sup>. ANSYS Fluent simulated a 51.4 mm diameter, 5 mm thick, 304 mm long stainless-steel pipe. Results showed increased turbulence and eddy formation. Analysis revealed higher convective heat transfer coefficient, pressure drop, and Nusselt number with increasing Reynolds number. Nusselt number also increased with 1–3 mm ball diameter. 6% porosity increase reduced pressure drop by 84.4%. Nusselt number rose by 46.7% (Reynolds 3,200–6,500) and 4.36% (heat flux 6,250–12,500 W m<sup>-2</sup>).

**Keywords:** Reynolds number; stainless steel balls; turbulent flow; Nusselt number; pressure drop; computational fluid dynamics

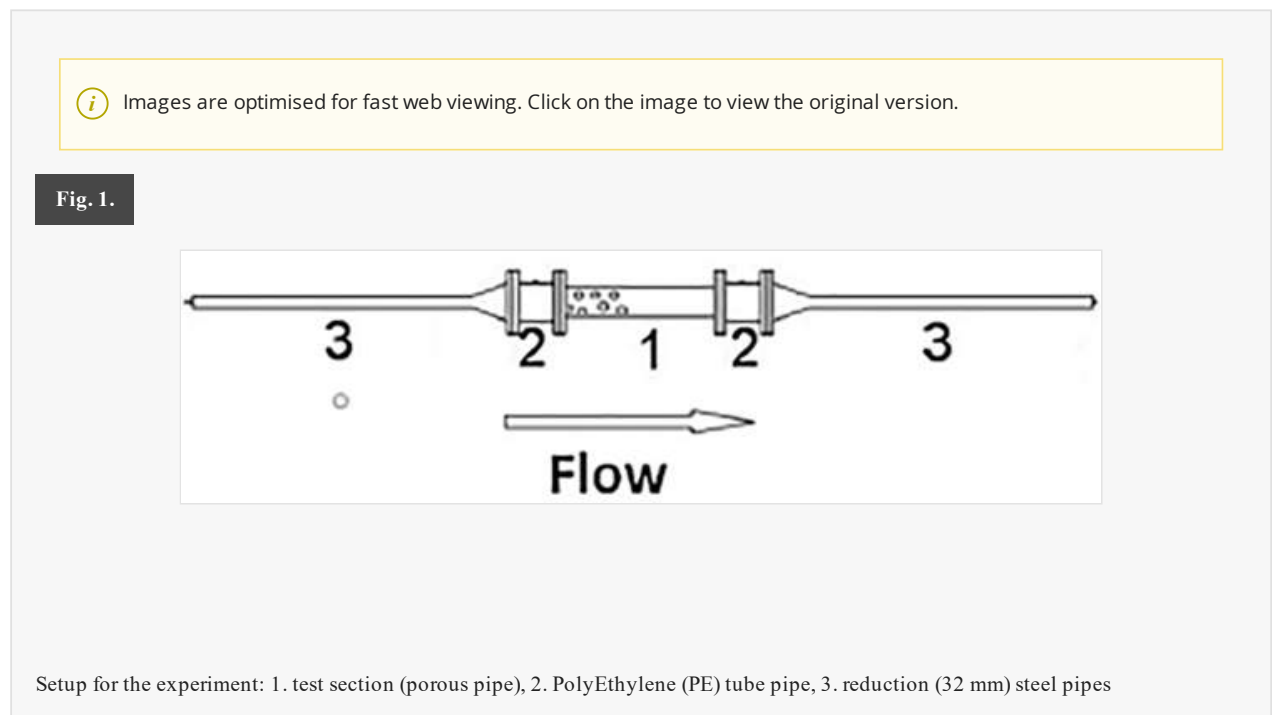
## 1 Introduction

For many technical applications, many approaches for using fins and baffles to improve heat transfer have been proposed. The use of porous media is another method for increasing heat transfer properties in industrial applications. Porous media can be characterized by their mechanical properties like porosity, permeability, and other characteristics. Porosity and permeability are two of the most important characteristics to consider when classifying porous material [1]. When a porous media is used as a hindrance in the fluid stream, heat transfer is enhanced. It is also necessary to minimize the pressure drop caused by these turbulences, which increases friction factor and heat exchanger thermal performance. Forced convection in a circular pipe packed with saturated porous medium and having a uniform heat flux at the wall is evaluated numerically and experimentally in several studies [2–8]. Porous mediums have been studied numerically with consideration of Local Thermal Non-Equilibrium (LTNE) conditions [9]. Various boundary conditions, as is apparent, can produce different results. Numerous studies have been carried out numerically on the phenomenon of pore flow in a specially designed porous medium [10–12]. 3D turbulent flow and thermal fields were studied for packed columns containing spheres and ellipsoids in various packing patterns [13]. Turbulence effects were included in governing equations by using the ReNormalization Group (RNG) theory  $k$ - $\epsilon$  model. Similar physical conditions resulted in maximum and minimum overall heat transfer efficiencies for the spherical filling and flat ellipsoidal filling arrangements, respectively. Heat transfer in a pipe filled with 3 mm-diameter steel balls were investigated experimentally and numerically [14]. The pipe's outer surface is heated at 7.5 kW m<sup>-2</sup>. A wide-ranging of Reynolds numbers is studied in the experiments (150–500). With commercial software Comsol, the Brinkman-Forchheimer is used to explore flow in porous media and the Navier-Stokes equations in the flow region. Results are shown by the temperature distribution along the pipe, the velocity distribution at the pipe's outlet, and the

difference in Nusselt numbers. An investigation of the flow and heat transfer properties of a pipe packed with the porous medium was carried out. A porous medium is created by using packed steel balls, and the fluid under study is water. The Reynolds number has been investigated with flow and heat transfer properties. The graphical representation of flow temperature variation at the middle of the plain for various Reynolds numbers is shown [15]. In a circular pipe study with steel balls as porous material during forced convection and utilizing water as a working medium with a uniform heat flux has been experimentally investigated. They find out how porosity, area, and position affect the Nusselt number. Porosity values and porous media were arranged in two different ways (0.44 and 0.45). Using a 55 mm diameter section with a porosity of 44%, the researchers found a significant increase in heat transfer efficiency in comparison to a clean flow case [16]. Another study was implemented the thermal conductivity and pressure loss of metallic porous medium fillings. As size decreases, the friction factor increases. Dendritic particles have lower heat transfer coefficients than spherical ones [17]. In the present work, the turbulent developing forced-convection flow and heat transfer of water flowing inside a circular pipe filled with stainless steel balls with varying porosity and heated symmetrically with variable heat flux ( $6,250, 12,500 \text{ W m}^{-2}$ ) for each case and velocity numerous from  $0.0626 \text{ m s}^{-1}$  to  $0.1272 \text{ m s}^{-1}$ . The simulation was performed with ANSYS Fluent 2022 R1 then validation with experimental results has been conducted. At constant Reynolds number, both the Nusselt number and friction factor exhibit an increase with an increase in the inclination angle for both the CuO–Ethylene Glycol/Water (EGW) nanofluid and the base fluid. Notably, the Nusselt number for the CuO–EGW nanofluid in the tube with a  $75^\circ$  rib bottom angle demonstrates an average increase of 135.8% compared to that in a smooth tube as reported in Wang et al. [18].

## 2 Problem statement

Figure 1 shows a stainless-steel circular tube measuring 51.4 mm in diameter, a thickness of 5 mm, and 304 mm in length. The temperature was set at 292 K, and a steady heat flux was applied to the wall. Polyethylene tubes, 51.4 inlets mm in diameter and 200 mm long, were joined to either side of the test section and used to create two porous materials by packing the pipe with 1 or 3 mm diameter stainless steel (AISI 304) balls. Since the flow is presumed to be constant, some assumptions have to be made to build the model. Two-dimensional (2D) axisymmetric flow is incompressible, turbulent, homogenous, and saturation with a single-phase fluid. In the porous zone, the fluid and solid phases are assumed to be in the same condition.



## 3 Porous media properties

### 3.1 Porosity ( $\emptyset$ )

The porous medium depends on the test section's and stainless-steel balls' diameters. It was easy to determine the porosity of each medium because the weight of the balls and the volume of the test section were known. The 1 and 3 mm spheres have porosities of 0.3690 and 0.3912, respectively [19].

### 3.2 Permeability ( $\alpha$ )

The porous medium's permeability is a characteristic that measures the fluid's capacity and ability to pass through it. It is defined by  $\alpha$  [20]:

$$\alpha = \frac{D_b^2 \emptyset^3}{36k(1 - \emptyset)^2}, \quad (1)$$

where  $D_b$  is the balls diameter,  $\emptyset$  is the porous medium's porosity, and  $\kappa$  is the Carman–Kozeny constant.

### 3.3 Pressure drop and friction factor

In theory of Vafai and Tien [21] proposed an empirical relationship based on porosity and pipe diameter  $D$  to describe the pressure drop for porous medium:

$$\frac{\Delta P}{L} \frac{D^2}{\mu u_m} = \frac{D^2}{\alpha} + \frac{FD}{\sqrt{\alpha}} \text{Re}, \quad (2)$$

where the pressure drops per unit length of the pipe ( $\Delta P/L$ ) to various fluid and pipe properties, including diameter ( $D$ ), viscosity ( $\mu$ ), thermal diffusivity ( $\alpha$ ), and Reynolds number (Re), as well as the Fanning friction factor ( $f$ ) and the average velocity of the fluid ( $u_m$ ).

Murshed et al. [22] expressed the pressure drop in terms of friction factor. The friction factor in channels for constant flows is known as:

$$f = \frac{2D\Delta P}{\rho u_m^2 L} = \frac{2D^2/\alpha}{\text{Re}} + \frac{2DF}{\sqrt{\alpha}}, \quad (3)$$

where  $\rho$  is fluid density.

### 3.4 Reynolds number (Re)


This dimensionless quantity indicates the relative importance of inertial forces to viscous forces in a fluid flow, and is known as [23, 24]:

$$\text{Re} = \frac{\rho u_m D_p}{\mu}. \quad (4)$$

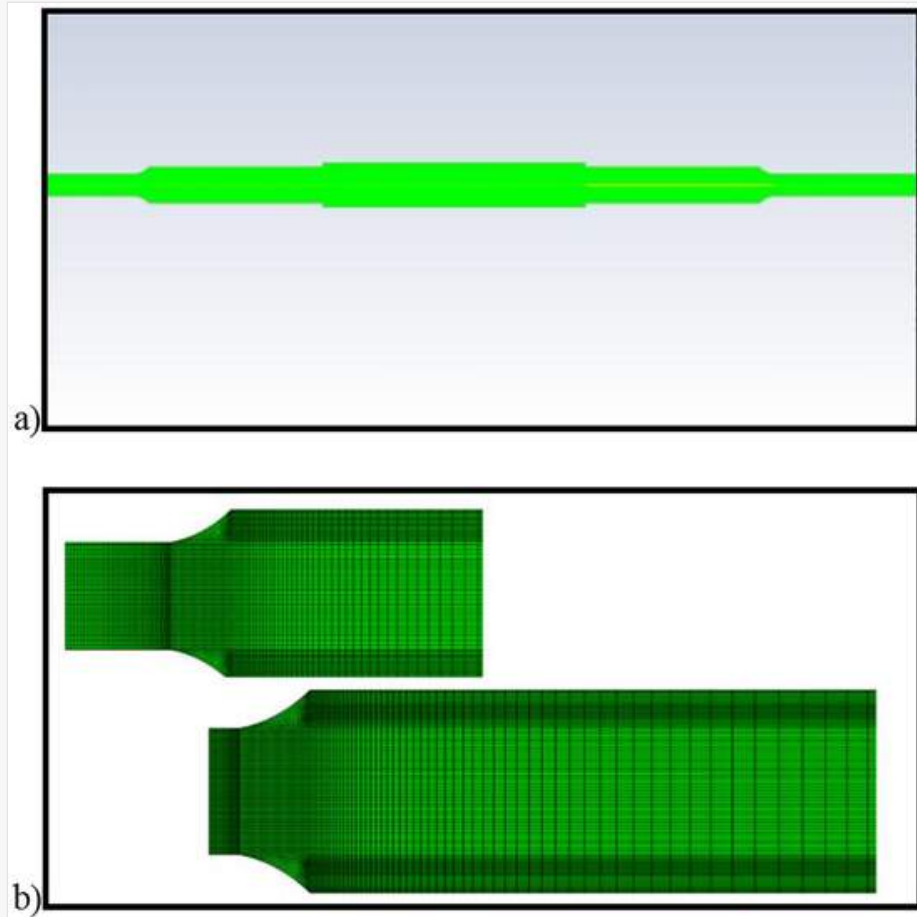
## 4 Numerical solution

Reynolds-Averaged Navier-Stokes (RANS) based simulations were run on ANSYS Fluent 2022 R1 with 2D axisymmetric simulations. Models for the numerical study, the realizable  $k-\varepsilon$  turbulence model (Enhanced Wall Treatment) is employed. Figure 2a shows the pipe geometry and coordinates system used in this investigation, with two-dimensional cylindrical coordinates being used ( $x, y$ ). Due to the flow domain's geometry, an axisymmetric state is selected. Using a 52,350 elements physics-controlled mesh provides the most accurate results. As it can be seen in Fig. 2b, the meshing gets even finer as you get closer to the wall. Determine, which sorts of element meshes will provide the desired levels of solution accuracy, convergence, and low run time. The following fluid and porous medium properties are used to specify boundary conditions: The constant temperature at the input is set at 292 K. Water enters the inlet at the same velocity. The boundary condition at the pipe's outlet section is referred to as a pressure outlet. Based on the flow, the pressure outlet boundary condition defines an outflow condition. The heat flux has been

constant along the top wall of the test section. Both the inlet and output sections' walls are insulated. In the hydraulic boundary condition, the flow was forced convection turbulent flow, fully developed flow, and no slip wall. The same parameters are used as in Bağcı et al. [19] experiment is utilized. The simulation is done on a PC with an Intel Core I i7-3610QM CPU @ running Windows 10 at 2.30 GHz.

 Images are optimised for fast web viewing. Click on the image to view the original version.

**Fig. 2.**



a) Geometry, b) mesh the porous pipe (test section)

#### 4.1 Model validation

To validate the existing model, the numerical results generated by ANSYS Fluent 2022 R1 software were compared to experimental results. Bağcı et al. [19] studied water movement inside stainless-steel balls of 1 and 3 mm diameters. There was 36% porosity in the porous mediums in both cases. The data encompass a wide range of Reynolds numbers, allowing for the inclusion of many significant flow regimes. In each ball's diameter, various values of porosity, permeability, and Forshheimer's modulus ( $F_m$ ) were listed in porous media and summarized in Table 1. As a result of this research, there appears to be even more differences in the available data on pressure drop and friction factor in spherical beds.

Table 1.

*i* The table layout displayed in this section is not how it will appear in the final version. The representation below is solely purposed for providing corrections to the table. To view the actual presentation of the table, please click on the [PDF](#) located at the top of the page.

Properties of porous media on the basis of [18]

Ball Diameter $D_b$ (mm)	Porosity $\emptyset$	Permeability $\alpha \times 10^{10} \text{ m}^2$	Forsheimer's modulus $F_m$
1	0.3690	$0.8451 \cdot 10^{-9}$	0.598
3	0.3912	$8.968 \cdot 10^{-10}$	0.586

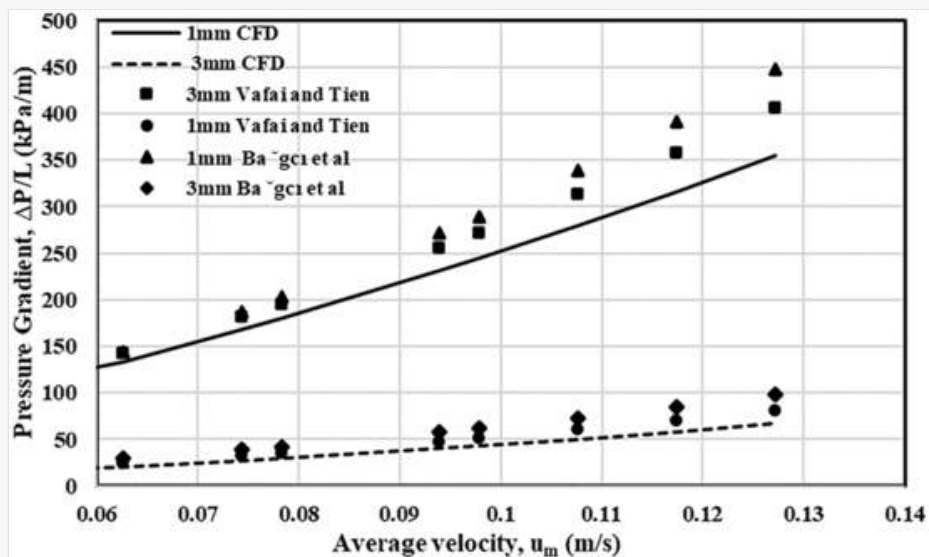
## 5 Result and discussion

In numerical investigations, different sets of inserts have produced varied results. Changing Nusselt number and pressure drop due to a change in velocities (Reynolds number). The change in pressure drop, and Nusselt number with Reynolds number can be graphed using this numerical data. When Reynolds numbers ranged from 3,200 to 6,500, heat flux values varied from 6,250 to 12,500  $\text{W m}^{-2}$ , and the use of porous inserts resulted in higher heat transfer. In addition, it was found that as heat flux increases, so does the temperature of the wall.

Figures 3 and 4 the pressure drop Friction factor decreases as the porosity increases. This was due to the combination of viscous and turbulent forces in a densely packed pipe.

*i* Images are optimised for fast web viewing. Click on the image to view the original version.

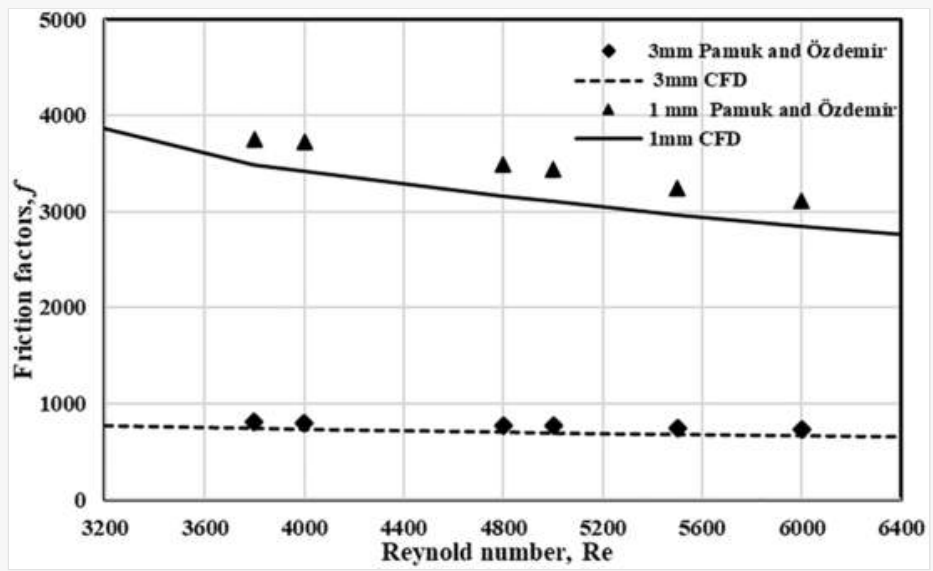
Fig. 3.



Pressure drop per length of pipe compared with average velocity for 1, 3 mm balls

*i* Images are optimised for fast web viewing. Click on the image to view the original version.

Fig. 4.



Friction factor per length of pipe compared with Reynolds number for 1, 3 mm balls

Figure 5 for a given heat flux and ball diameter, the pressure drop rises as the Reynolds number rises. Figure 6 the surface Nusselt number rises as the Reynolds number, heat flux rises and porosity decreases. As it can be observed, the Nusselt number for  $D_b = 1$  mm is the highest because of the larger contact area and the smallest porosity 0.3690 compared to 0.3912 for the  $D_b = 3$  mm, this is the case. The small diameter of the balls leads to a narrow passageway, low velocity, and channeling. Balls having a diameter of between (1–3 mm) minimize heat transfer when placed close to the wall.


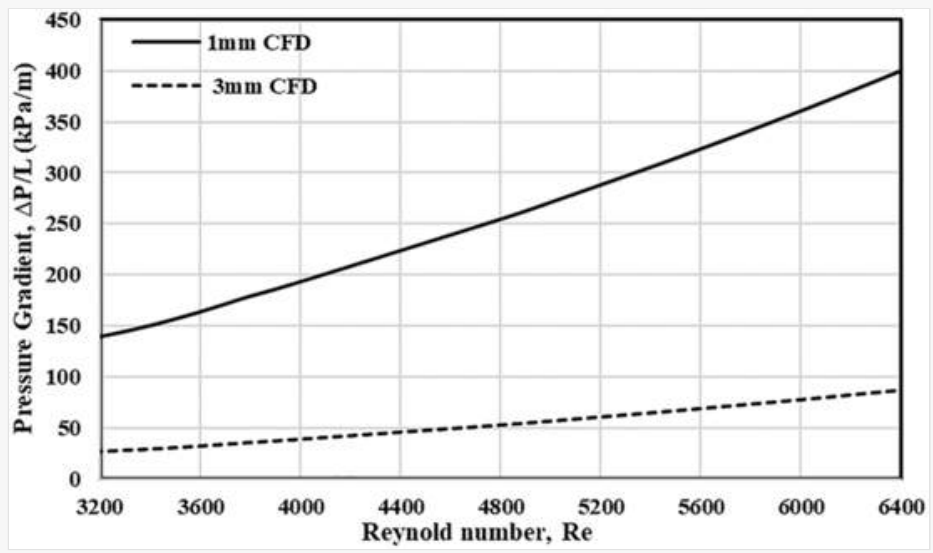

 Images are optimised for fast web viewing. Click on the image to view the original version.

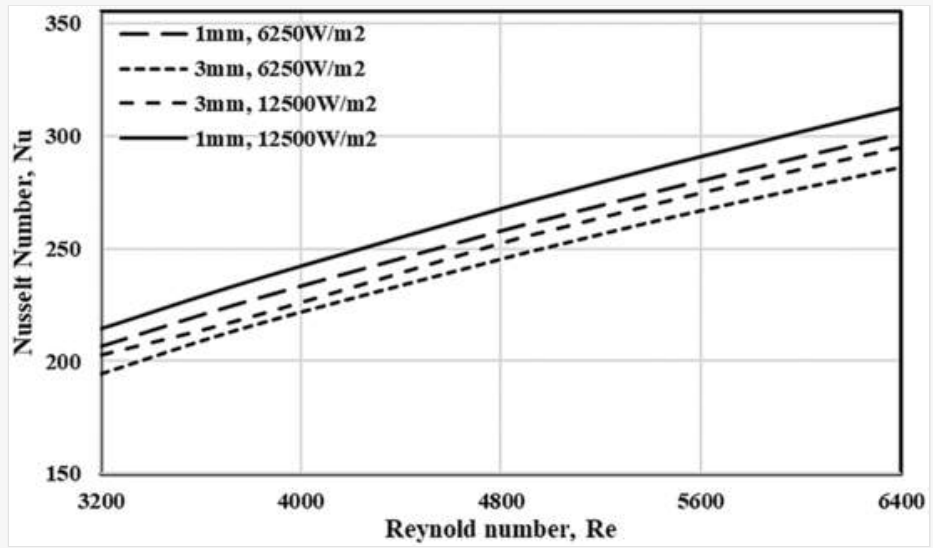
Fig. 5.



Pressure drops vs. Reynolds numbers and porosity

 Images are optimised for fast web viewing. Click on the image to view the original version.

**Fig. 6.**



Nusselt number vs. Reynolds numbers for 1, 3 mm balls

As in Fig. 7 the Reynolds number decreases and heat flux increases, the wall temperature along test section is increased. In Fig. 8 the results of the distribution of wall temperature, pressure drop, heat transfer coefficient, Nusselt number along the length of the test pipe at Reynolds number 3,200 and heat flux 6,250 W m<sup>-2</sup> for 3 mm balls.


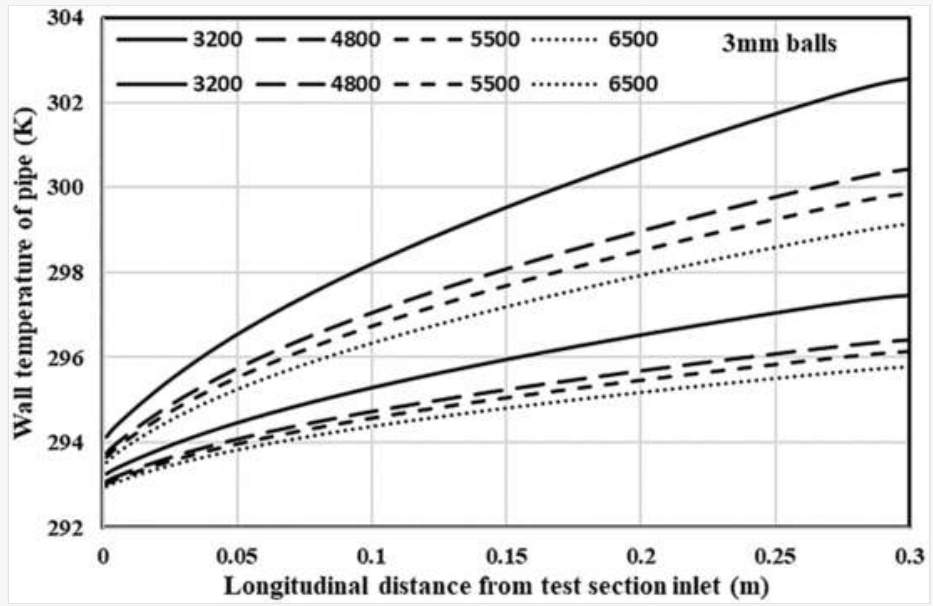

 Images are optimised for fast web viewing. Click on the image to view the original version.

Fig. 7.

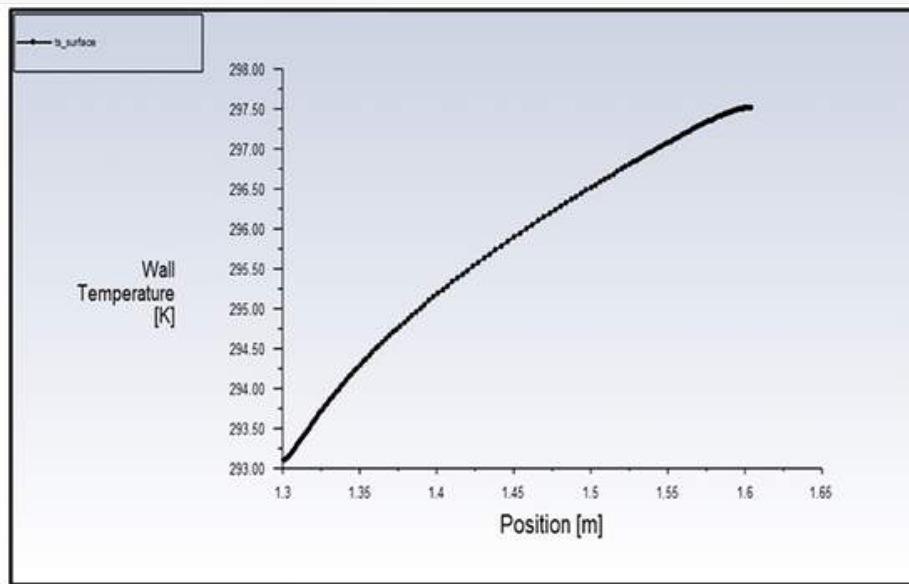




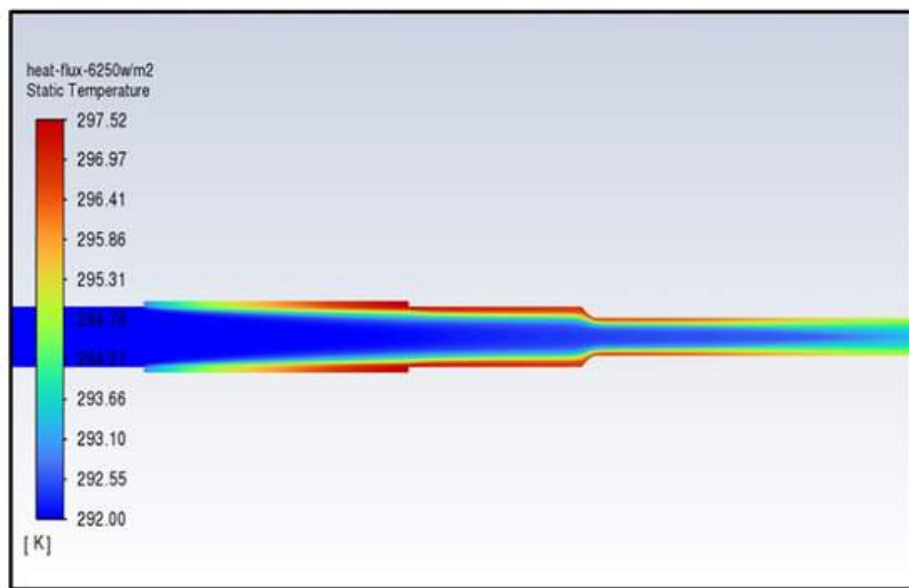
Wall temperature distributions per length of pipe compared with Reynolds numbers for heat flux 6,250, 12,500  $W m^{-2}$

 Images are optimised for fast web viewing. Click on the image to view the original version.

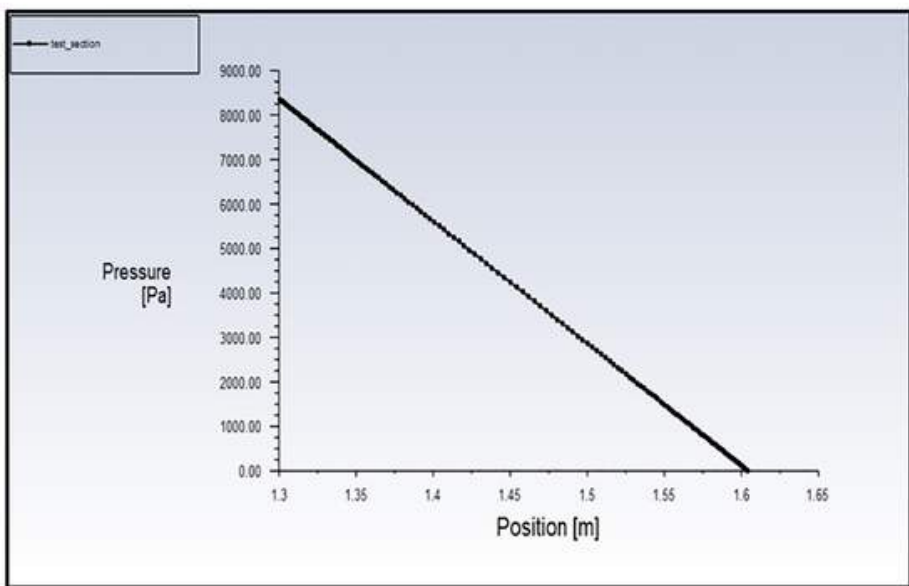
**Fig. 8.**



a) Wall temperature curve for selected section




b) Wall temperature contour

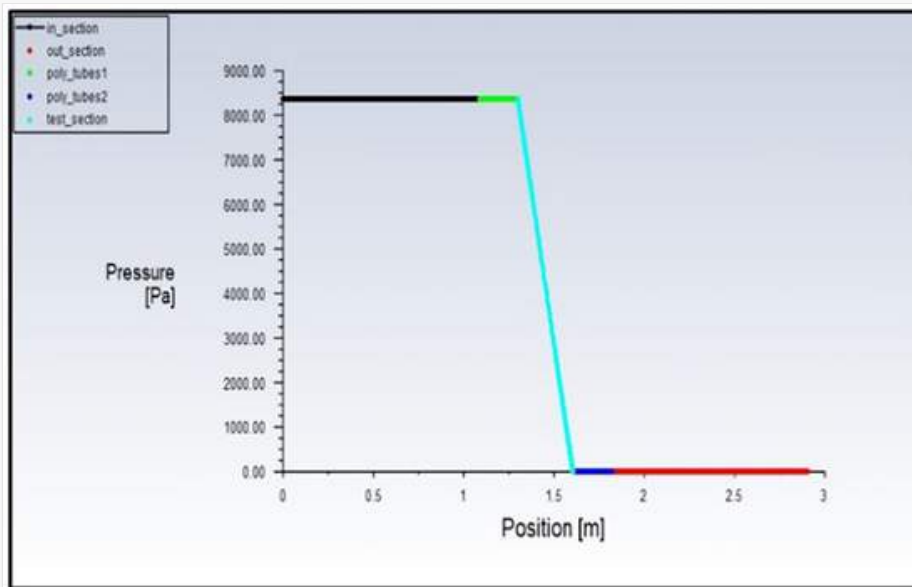


c) Wall temperature contour

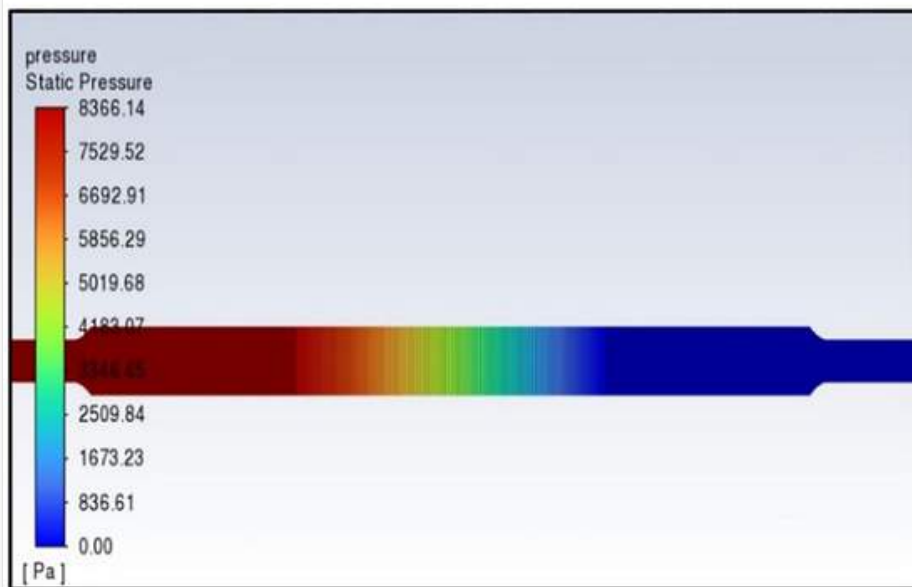
The results of the distribution of wall temperature, pressure drop, heat transfer coefficient, Nusselt number along the length of the test pipe at Reynolds number 3,200 and heat flux  $6,250 \text{ W m}^{-2}$  for 3 mm balls

 Images are optimised for fast web viewing. Click on the image to view the original version.

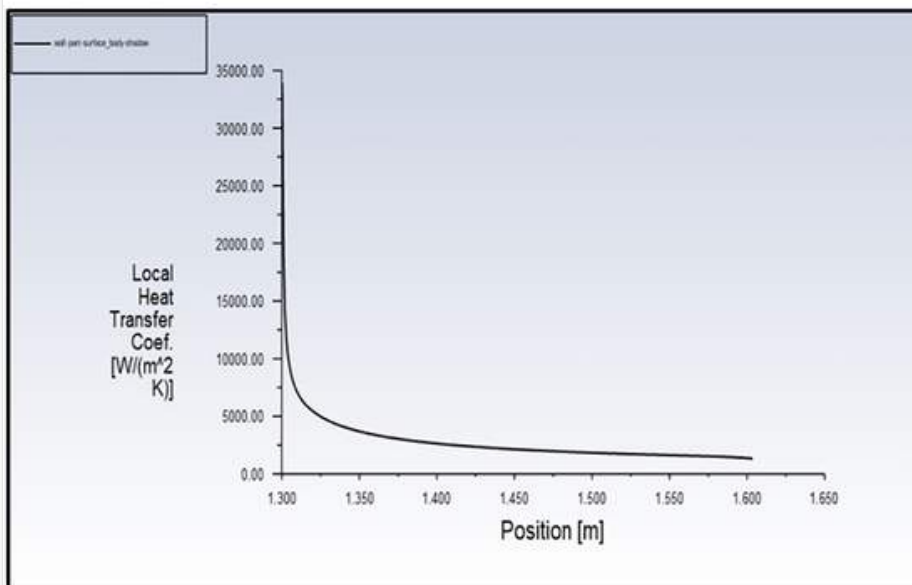
**Fig. 8.**



d) Pressure drop curve for selected pipe

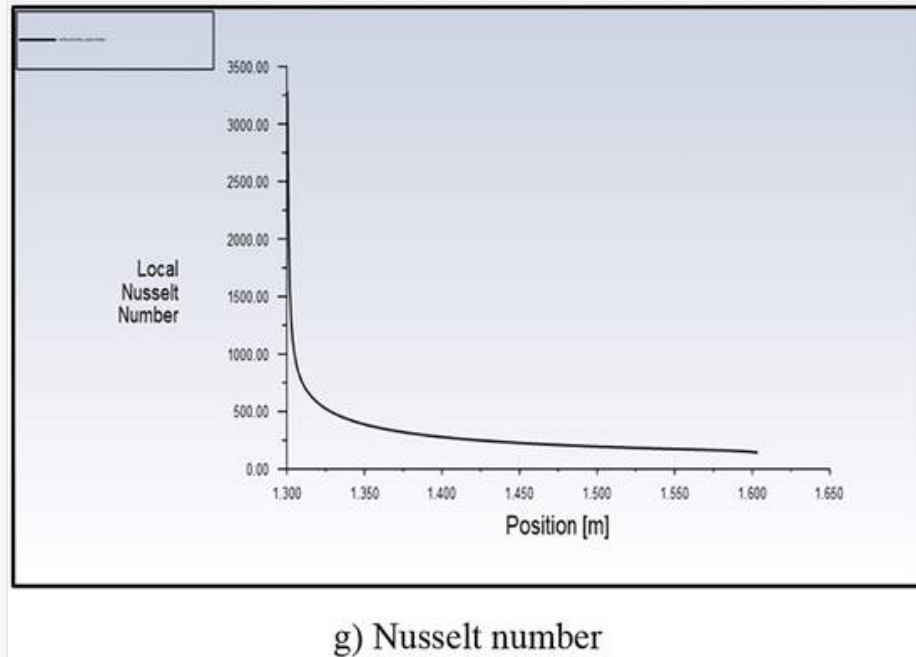


e) Pressure contour



f) Heat transfer coefficient

Fig. 8.




Continued

## 6 Conclusion

In this study the flow in a horizontal porous pipe subjected to a constant heat flux boundary condition was quantitatively characterized. Increases in Reynolds number and heat flux lead to an increase in the surface Nusselt number and surface heat transfer coefficient. When the porosity of a pipe increases from 0.3690 to 0.3912, the pressure drops decrease by 84.4%. This is to be expected, since the packing is denser in the case of a balls with a diameter of 1 mm, Nusselt number increased by 46.7% with an increase in Reynolds number from 3,200 to 6,500 while increased 4.36% with an increase in heat flux from 6,250 to 12,500 W m<sup>-2</sup>. The highest wall temperature occurs at 3 and 1 mm balls diameter, respectively. The study shows an increase in the wall temperature at higher heat flux values 12,500 W m<sup>-2</sup>. At constant heat flux, the surface heat transfer coefficient increases with the increase Reynolds number, the adding of stainless-steel balls in the pipe caused an increase in fluid temperature, the size of ball diameter has a significantly larger influence on the value of porosity. Surface heat transfer coefficients and surface Nusselt number **Q5** increase as stainless-steel ball diameter decreased.

## References

 The corrections made in this section will be reviewed by journal production editor.

- [1] A. M. Saleh, S. A. Rasheed, and R. B. Smasem, "Convection heat transfer in a channel of different cross section filled with porous media," *Kufa J. Eng.*, vol. 9, no. 2, pp. 57-73, 2018.
- [2] A. M. Hussein, "A theoretical study of laminar free convection through porous trombe wall with passive solar energy," *J. Tech.*, vol. 21, no. 1, pp. A140-150, 2008.
- [3] B. Mohamad and A. Zelentsov, "1D and 3D modeling of modern automotive exhaust manifold," *J. Serbian Soc. Comput. Mech.*, vol. 13, no. 1, pp. 80-91, 2019.

[4]

C. Yang, W. Liu, and A. Nakayama, "Forced convective heat transfer enhancement in a tube with its core partially filled with a porous medium," *Open Conserv. Biol. J.*, vol. 1, pp. 1-6, 2009.

- [5] Z. F. Huang, A. Nakayama, K. Yang, C. Yang, and L. Wei, "Enhancing heat transfer in the core flow by using porous medium insert in a tube," *Int. J. Heat Mass Transfer*, vol. 53, nos 5-6, pp. 1164-1174, 2010.
- [6] T. A. Tahseen, "An experimental study for mixed convection through a circular tube filled with porous media and fixed horizontally and inclined," *Mod. Appl. Sci.*, vol. 5, no. 2, pp. 128-142, 2011.
- [7] M. A. Teamah, W. M. El-Maghlany, and M. M. K. Dawood, "Numerical simulation of laminar forced convection in horizontal pipe partially or completely filled with porous material," *Int. J. Therm. Sci.*, vol. 50, no. 8, pp. 1512-1522, 2011.
- [8] M. T. Pamuk and M. Özdemir, "Heat transfer in porous media of steel balls under oscillating flow," *Exp. Therm. Fluid Sci.*, vol. 42, pp. 79-92, 2012.
- [9] B. Alazmi and K. Vafai, "Constant wall heat flux boundary conditions in porous media under local thermal non-equilibrium conditions," *Int. J. Heat Mass Transfer*, vol. 45, no. 15, pp. 3071-3087, 2002.
- [10] G. M. Porta, S. Chaynikov, J. F. Thovert, M. Riva, A. Guadagnini, and P. M. Adler, "Numerical investigation of pore and continuum scale formulations of bimolecular reactive transport in porous media," *Adv. Water Resour.*, vol. 62, Part B, pp. 243-253, 2013.
- [11] P. Kundu, V. Kumar, Y. Hoarau, and I. M. Mishra, "Numerical simulation and analysis of fluid flow hydrodynamics through a structured array of circular cylinders forming porous medium," *Appl. Math. Model.*, vol. 40, nos 23-24, pp. 9848-9871, 2016.
- [12] S. Baragh, H. Shokouhmand, S. S. M. Ajarostaghi, and M. Nikian, "An experimental investigation on forced convection heat transfer of single-phase flow in a channel with different arrangements of porous media," *Int. J. Therm. Sci.*, vol. 134, pp. 370-379, 2018.
- [13] J. Yang, Q. Wang, M. Zeng, and A. Nakayama, "Computational study of forced convective heat transfer in structured packed beds with spherical or ellipsoidal particles," *Chem. Eng. Sci.*, vol. 65, no. 2, pp. 726-738, 2010.
- [14] M. T. Pamuk, "Numerical study of heat transfer in a porous medium of steel balls," *Therm. Sci.*, vol. 23, no. 1, pp. 271-279, 2019.
- [15] F. Qader, A. M. Hussein, S. H. Danook, and B. Mohamad, "Enhancement of double-pipe heat exchanger effectiveness by using porous media and TiO<sub>2</sub> water," *CFD Lett.*, vol. 15, no. 4, pp. 31-42, 2023.
- [16] S. M. M. Reddy, V. M. Kulkarni, S. Jain, S. A. Kumar, and K. Manjunatha, "An experimental investigation of heat transfer performance for forced convection of water in a horizontal pipe partially filled with a porous medium," *Int. Org. Sci. Res. J. Mech. Civ. Eng.*, vol. 13, no. 4, pp. 131-140, 2016.
- [17] W. Tu, Y. Wang, and Y. Tang, "Thermal characteristic of a tube fitted with porous media inserts in the single-phase flow," *Int. J. Therm. Sci.*, vol. 110, pp. 137-145, 2016.
- [18] W. Wang, B. Zhang, L. Cui, H. Zheng, J. Klemeš, and J. Wang, "Numerical study on heat transfer and flow characteristics of nanofluids in a circular tube with trapezoid ribs," *Open Phys.*, vol. 19, no. 1, pp. 224-233, 2021.
- [19] Ö. Bağcı, N. Dukhan, and M. Özdemir, "Flow regimes in packed beds of spheres from pre-Darcy to turbulent," *Transport Porous Media*, vol. 104, no. 3, pp. 501-520, 2014.

- [20] S. Amroune, A. Belaadi, M. Zaoui, N. Menaseri, B. Mohamad, K. Saada, and R. Benyettou, "Manufacturing of rapid prototypes of mechanical parts using reverse engineering and 3D printing," *J. Serbian Soc. Comput. Mech.*, vol. 15, no. 1, pp. 167-176, 2021.
- [21] K. Vafai and C. L. Tien, "Boundary and inertia effects on flow and heat transfer in porous media," *Int. J. Heat Mass Transf.*, vol. 24, no. 2, pp. 195–203, 1981.
- [22] S. M. S. Murshed, K. C. Leong, and C. Yang, "Thermophysical and electrokinetic properties of nanofluids – A critical review," *Appl. Therm. Eng.*, vol. 28, nos 17–18, pp. 2109-2125, 2008.
- [23] L. Bytčanková, J. Rumann, and P. Zubik, "Comparative study of LDA and PIV methods for flow homogeneity measurements," *Pollack Period.*, vol. 17, no. 3, pp. 106-110, 2022.
- [24] M. Osfoury and A. Simon, "Study on the thermal conductivity and density of foam glass," *Pollack Period.*, vol. 18, no. 1, pp. 126-131, 2023.

## Queries and Answers

Q1

**Query:** Please note that as per style, the ORCID information is recommended for the corresponding author. Hence, please provide ORCID for the corresponding author "Barhm Mohamad". Refer to the site "<https://orcid.org/>" for more information about ORCID.

**Answer:** <https://orcid.org/0000-0001-8107-6127>

Q2

**Query:** Please confirm that given names and surnames have been identified correctly and are presented in the desired order and please carefully verify the spelling of all authors' names. Please note that changes in authorship are not allowed in this stage.

**Answer:** Confirm

Q3

**Query:** Please check the accuracy of the affiliations of each author and make changes as appropriate. Affiliations cannot be changed once the article has been published online.

**Answer:** Confirm

Q4

**Query:** Please confirm that the provided email "[barhm.mohamad@epu.edu.iq](mailto:barhm.mohamad@epu.edu.iq)" is the correct address for official communication; else provide an alternate e-mail address to replace the existing one.

**Answer:** The email are correct

**Query:** Please check acknowledgment/funding information and make sure none is missing and those listed – if any – are accurate. Once the article is published these can only be added/updated in a corrigendum.

**Answer:** There is no acknowledgment/funding information in this article.